Since January 2020 Elsevier has created a COVID-19 resource centre with free information in English and Mandarin on the novel coronavirus COVID-19. The COVID-19 resource centre is hosted on Elsevier Connect, the company's public news and information website.

Atmospheric Pollution Research 13 (2022) 101510

Contents lists available at ScienceDirect

Atmospheric Pollution Research

journal homepage: www.elsevier.com/locate/apr

Local and transboundary impacts of $PM_{2.5}$ sources identified in Seoul during the early stage of the COVID-19 outbreak

Youngkwon Kim [a,b], Kwonho Jeon [c], Jieun Park [d], Kyuseok Shim [e], Sang-Woo Kim [e], Hye-Jung Shin [f], Seung-Muk Yi [a,d,*], Philip K. Hopke [g,h]

[a] Department of Environmental Health Sciences, Graduate School of Public Health, Seoul National University, 1 Gwanak-ro, Gwanak-gu, Seoul, 08826, Republic of Korea
[b] Division of Policy Research, Green Technology Center, Seoul, 04554, Republic of Korea
[c] Climate and Air Quality Research Department Global Environment Research Division, National Institute of Environmental Research, Incheon, Republic of Korea
[d] Institute of Health and Environment, Seoul National University, 1 Gwanak-ro, Gwanak-gu, Seoul, 08826, Republic of Korea
[e] School of Earth and Environmental Sciences, Seoul National University, 1 Gwanak-ro, Gwanak-gu, Seoul, 08826, Republic of Korea
[f] Air Quality Research Division, National Institute of Environmental Research, Incheon, Republic of Korea
[g] Center for Air Resources Engineering and Science, Clarkson University, Potsdam, NY, 13699, USA
[h] Department of Public Health Sciences, University of Rochester, School of Medicine and Dentistry, Rochester, NY, 14642, USA

ARTICLE INFO

Keywords:
$PM_{2.5}$
COVID-19
Source apportionment
Dispersion normalized PMF
Transboundary pollution

ABSTRACT

Countries in Northeast Asia have been regulating $PM_{2.5}$ sources and studying their local and transboundary origins since $PM_{2.5}$ causes severe impacts on public health and economic losses. However, the separation of local and transboundary impacts is not fully realized because it is impossible to change air pollutant emissions from multiple countries experimentally. Exceptionally, the early stage of the COVID-19 outbreak (January–March 2020) provided a cross-country experiment to separate each impact of $PM_{2.5}$ sources identified in Seoul, a downwind area of China. We evaluated the contributions of $PM_{2.5}$ sources compared to 2019 using dispersion normalized positive matrix factorization (DN-PMF) during three meteorological episodes. Episodes 1 and 2 revealed transboundary impacts and were related to reduced anthropogenic emissions and accumulated primary pollutants in Northeast China. Anthropogenic emissions, except for the residential sector, decreased, but primary air pollutants accumulated by residential coal combustion enhanced secondary aerosol formation. Thus, the contributions of sulfate and secondary nitrate increased in Seoul during episode 1 but then decreased maximally with other primary sources (biomass burning, district heating and incineration, industrial sources, and oil combustion) during episode 2 under meteorological conditions favorable to long-range transport. Local impact was demonstrated by atmospheric stagnation during episode 3. Meteorological condition unfavorable to local dispersion elevated the contributions of mobile and coal combustion and further contributed to $PM_{2.5}$ high concentration events (HCE). Our study separates the local and transboundary impacts and highlights that co-operations in Northeast Asia on secondary aerosol formation and management of local sources are necessary.

1. Introduction

Fine particulate matter ($PM_{2.5}$) has severe impacts on public health (Apte et al., 2018; Cohen et al., 2017; Yang et al., 2022; Zhang et al., 2017), produces economic losses (Maji et al., 2018; Xie et al., 2016, 2019), and enhances the spread of coronavirus disease (COVID-19) (Ali et al., 2021; Borro et al., 2020; Rovetta and Castaldo, 2020) that has led most countries to set air quality standards for $PM_{2.5}$ (Czy, 2019; Kim and Lee, 2018; Pitiranggon et al., 2021; Zhang et al., 2019). High concentration events (HCEs) of $PM_{2.5}$ occur consistently in South Korea, during the cold season, including January to March, especially in the Seoul-Metropolitan area (SMA; 33 cities comprising Seoul, Incheon, and Gyeonggi province). The number of highly polluted days in Seoul with $PM_{2.5}$ concentration exceeding 75 $\mu g/m^3$ for more than 2 h was 10 in 2017, 18 in 2018, and 29 in 2019 (clean air.seoul.go.kr/statistics/warning/pm25) (Bae et al., 2019). and (Kim et al., 2020) observed

Peer review under responsibility of Turkish National Committee for Air Pollution Research and Control.
* Corresponding author. Department of Environmental Health Sciences, Graduate School of Public Health, Seoul National University, 1 Gwanak-ro, Gwanak-gu, Seoul, 08826, Republic of Korea.
E-mail address: yiseung@snu.ac.kr (S.-M. Yi).

https://doi.org/10.1016/j.apr.2022.101510
Received 19 April 2022; Received in revised form 14 July 2022; Accepted 14 July 2022
Available online 18 July 2022

that long-range transport of air pollutants from the Jing-Jin-Ji region (BTH; 28 cities comprising Beijing, Tianjin, and Hebei province) of China and the surrounding Northeastern China area played an essential role in haze formation in Seoul, Korea. However, reductions in emissions and improvements in air quality have been reported since 2013 in China, which is located in an upwind area relative to Seoul (Fan et al., 2020; Zhao et al., 2019). Long-term trend studies reported that $PM_{2.5}$ concentrations have not decreased in Korea since 2013 as local dispersion has weakened (Kim et al., 2017b; Kim et al., 2020). These results suggest that both local and transboundary impacts of $PM_{2.5}$ sources are important for air quality management in Korea.

To improve air quality, South Korea has been intensively reducing air pollutant emissions in transportation, industry, power generation, and residential sectors during the cold season by implementing the seasonal fine dust management program since December 2019 (www.blueskyday.kr). With regulations on emissions from $PM_{2.5}$ and precursor sources such as vehicles and coal combustion being implemented within South Korea, identifying the local and transboundary impacts of $PM_{2.5}$ sources in South Korea has become critical (Choi et al., 2019; Ministry of Environment Republic of Korea, 2019). However, in general, accurately estimating the transboundary impact of $PM_{2.5}$ sources is challenging due to the inability to manipulate source emissions from other countries and evaluate the impacts of those changes on South Korea.

Exceptionally, the early stage of the COVID-19 outbreak during January–March 2020 is an unprecedented period to evaluate the effects of China's reduced anthropogenic activities, downtime measures for factories, and regional containment measures on $PM_{2.5}$ concentration and source contributions in Seoul. In 2020, the outbreak of COVID-19 caused many of China's source emissions to be substantially reduced during the nationwide lockdown. To prevent the spread of the virus, the Chinese government closed the border of Wuhan City, Hubei Province on January 23, 2020. Subsequently, lockdown measures on a regional scale began gradually in Hubei Province, and full-scale lockdown measures on a national scale by the Chinese government were implemented beginning on January 25, 2020. From January 25, 2020, for about 30 days outdoor activities were restricted in 31 provinces in China (Tu et al., 2020), and a state of national emergency was declared on February 6, 2020. The border of Hebei Province closed from February 15 to March 25, 2020. Due to these measures, the reduction of anthropogenic activity and air pollutants emissions in China during the COVID-19 outbreak without precedent reduced air-pollutant emissions (Cui et al., 2020; Ming et al., 2020; Wang et al., 2020). Criteria air pollutants concentrations and the aerosol optical depth (AOD) sharply decreased in China and Korea (Chang et al., 2020a; Dai et al., 2020; Han et al., 2020; Le et al., 2020a; Zhao et al., 2020). COVID-related reductions in air pollutant emissions in China were greater than previous large-scale emission reduction efforts, such as Beijing Olympics 2008 and 2014 APEC (Zhang et al., 2021). These emissions reductions were considered to be the result of the maximum possible reductions in China. In the meantime, Korea implemented full-scale lockdown measures (social distancing) from March 22, 2020 to prevent the spread of COVID-19. However, air quality did not consistently improve in China during the lockdown due to local and transboundary impacts of $PM_{2.5}$ sources (Chang et al., 2020b; Dai et al., 2021a; Le et al., 2020b), and similar cases were reported in Spain and Thailand. (Briz et al., 2022; Wetchayont et al., 2021). These results can help understand the local and transboundary impacts of $PM_{2.5}$ sources by providing an unprecedented cross-country experiment.

This study focused on the early stage of the COVID-19 outbreak in 2020 (January–March 2020) when lockdown measures were implemented mainly in China, not South Korea to separate the local and transboundary impacts of $PM_{2.5}$ sources identified in Seoul. We evaluated the contributions of $PM_{2.5}$ sources relative to comparable periods in 2019 using dispersion normalized positive matrix factorization (DN-PMF) during three episodes showing the different meteorological patterns.

2. Material and methods

2.1. Sampling and analysis

Ground-based $PM_{2.5}$ monitoring and chemical speciation were conducted at supersites operated by the National Institute of Environmental Research (NIER) in Seoul. The supersite in Seoul is a residential and commercial complex located 6.3 km northwest of Seoul city center, adjacent to high traffic zones (Fig. S1). As mentioned in the introduction, Seoul was affected not only by long-range transported air pollutants but also by local primary source emissions in Korea. The supersite is about 25 km away from industrial facilities emitting SO_x (>4000 ton yr^{-1}) and agricultural areas burning biomass in Incheon and Gyeonggi Province during the cold season (Kim et al., 2017a). The northern area of the supersite had high $PM_{2.5}$ emissions from residential coal combustion (Fig. S1), suggesting that the sampling site was affected by local primary sources.

$PM_{2.5}$ mass concentrations were measured using the beta-ray attenuation method (BAM-1020, Met One, USA). Carbon species (organic carbon and elemental carbon: OC and EC) were measured using a carbon analyzer (thermal–optical transmittance method: Model-4 Semi-Continuous OC-EC Field Analyzer, Sunset Laboratory Inc., USA). Ionic species (SO_4^{2-}, NO_3^-, Cl^-, K^+, and NH_4^+) were measured using continuous monitoring equipment (ambient ion monitor (AIM): URG-9000D, URG Corp., USA). Trace elements (Si, Ca, Ti, V, Cr, Mn, Fe, Ni, Cu, Zn, As, Br, and Pb) were measured using an X-ray fluorescence spectrometry (XRF) (Xact 625i, COOPER ENVIRONMENTAL, USA). Hourly gaseous air pollutant data (ozone and nitrogen dioxide) were obtained from the National Ambient Air Quality Monitoring Information System (NAMIS) (Air Korea; airkorea.or.kr) (Table S1). Ground-based monitoring methods and data sources for China were obtained from MEE, China (see Supplementary Material Text S1 and Table S1).

2.2. Dispersion normalized positive matrix factorization (DN-PMF)

The hourly source contributions to $PM_{2.5}$ were quantitatively estimated by normalizing differences in meteorological conditions using DN-PMF (Dai et al., 2020). Source contributions estimated using conventional PMF, which have been widely used for source apportionment studies (Heo et al., 2009; Hopke, 2016; Lee et al., 1999), are affected by the dilution effect of atmospheric dispersion. DN-PMF apportions the source contributions by reducing the dilution effect by normalizing the data from each measurement period to the mean ventilation coefficient (VC: MLH × wind speed) over the entire monitoring period (Dai et al., 2021b) and reduces variations in concentrations due to the dilution effect in each period. The equation for calculating VC_i of ith sample measurement time as (Ashrafi et al., 2009):

$$VC_i = MLH_i \times \overline{u_i} \quad (1)$$

Here, MLH_i and $\overline{u_i}$ indicate average MLH and wind speed, respectively, during i time interval. DN-PMF normalizes the concentration of input data using VC as follows:

$$C_{vc,\,i} = C_i \times \frac{VC_i}{VC_{mean}} \quad (2)$$

Here, $C_{vc,\,i}$ indicates the normalized concentration of C_i during i time interval, C_i is concentration measured during i time interval, and VC_{mean} is the VC average value of the total sampling period. The uncertainties in the input composition data were estimated according to the PMF 5.0 User Guide (US EPA, 2014). The QA/QC of DN-PMF input data was provided in the Supplementary Material (Text S2). After the source profile and contributions were resolved from the dispersion-normalized data, $PM_{2.5}$ concentrations and source contributions were unnormalized based on the normalization ratio to reproduce the original monitoring data.

2.3. Meteorological data analysis

Synoptic meteorological patterns were analyzed to select episodes with meteorological conditions favorable to long-range transport or local stagnation of air pollutants. European Center for Medium-Range Weather Forecasts (ECMWF) Reanalysis version 5 (ERA 5) data with 30 km grid resolution and 137 vertical levels (Hersbach et al., 2020) (https://confluence.ecmwf.int/) were used to investigate the synoptic meteorological patterns for selected episodes (Bey et al., 2001). To further identify potential source locations and group similar air masses origins, the potential source contribution function (PSCF) and cluster analysis of backward trajectories were performed. Backward trajectories were analyzed using reanalysis data (ftp://arlftp.arlhq.noaa.gov/archives) provided by the national oceanic and atmospheric administration (NOAA). Also, the Conditional bivariate probability function (CBPF) was applied to identify local source locations (Uria-tellaetxe and Carslaw, 2014). CBPF and cluster analysis were calculated using the 'openair' package of R Studio (version 4.1.2). Detailed descriptions of PSCF and CBPF were provided in the Supplementary Material (Text S3-4) (Table S1). Ground-based meteorological monitoring in Seoul was conducted with an Automated Synoptic Observing System (ASOS), which is managed by Korea Meteorological Administration (KMA) (https://data.kma.go.kr/). The mixing layer height (MLH) in Seoul was estimated from ground-based elastic aerosol lidar as part of Korea Aerosol LIDAR Observation Network (KALION) (http://www.kalion.kr/) (Park et al., 2021).

2.4. Statistical analysis

The target data for statistical analysis in this study are $PM_{2.5}$ concentration and source contribution data based on ambient samples, and these data are not characterized by a normal distribution and equal variance. This study statistically evaluated the differences in $PM_{2.5}$ concentrations and source contributions between 2020 and 2019 using Mann-Whitney *U* test. Mann-Whitney *U* test is an analytical method that compares two independent groups that are not normally distributed (Mann and Whitney, 1947). This method statistically compares two groups of samples with no assumptions about the type of distribution (i.e., normal, lognormal, exponential, etc.) (Helsel et al., 2002).

Annual differences between $PM_{2.5}$ concentrations during 2016–2019 were assessed statistically by the Kruskal-Wallis ANOVA on ranks (Kruskal and Wallis, 1952). Kruskal-Wallis test is an analytical method that compares three or more groups that are not normally distributed and independent. This method statistically compares sample groups using rank without any assumptions about the distribution of the population mentioned above. Statistical significance was estimated at three levels ($p < 0.001$, $p < 0.01$, $p < 0.05$). Mann-Whitney *U* test and Kruskal-Wallis test were performed using SigmaPlot (ver. 14.5).

3. Results and discussion

3.1. Monthly average of $PM_{2.5}$ concentrations in Korea and China

After the QA/QC procedure of ground-based monitoring data, the number of final Seoul data was 1081 and 846 in 2019 and 2020, respectively. The average concentration of $PM_{2.5}$ during the study period was 39.6 μg/m^3 (2019: 45.2 μg/m^3, 2020: 32.5 μg/m^3). As the first step in this study, we evaluated the changes in $PM_{2.5}$ concentrations in 2020 compared pairwise with those of the corresponding period in 2019 (after this, referred to as "compared to 2019″). The Lunar New Year had a holiday effect on anthropogenic activities (Fig. S2), these periods (2020: January 24–30, 2019: February 4–10) were excluded from the evaluation period. Before the evaluation, we statistically analyzed the distribution of $PM_{2.5}$ concentrations from 2016 to 2019 to check the trend of increasing or decreasing $PM_{2.5}$ concentrations in the past. As a result of Kruskal Wallis ANOVA on ranks, The concentrations of $PM_{2.5}$ show no continuous increases or decreases for more than two years in Seoul (Fig. S3). Therefore, this study focused on changes in $PM_{2.5}$ concentrations compared to the nearest 2019 from 2020. Average $PM_{2.5}$ concentrations in the BTH, Baengnyeong Island, and Seoul decreased from 108 to 61.9 μg/m^3 (−43%), 32.4 to 32.0 μg/m^3 (−1.19%), and 42.7 to 33.3 μg/m^3 (−22%), respectively in February 2020 compared to those in February 2019 (Fig. 1). After that, the average $PM_{2.5}$ concentrations in the BTH, Baengnyeong Island, and Seoul in March 2020 compared to those in March 2019 decreased from 54.4 to 45.1 μg/m^3 (−17%), 46.9 to 23.5 μg/m^3 (−50%), and 55.4 to 29.3 μg/m^3 (−47%), respectively. Conversely, the average $PM_{2.5}$ concentration increased from 53.0 to 63.0 μg/m^3 (+19%) in Beijing during February 2020 compared to 2019 and decreased from 52.0 to 35.0 μg/m^3 (−33%) during March. The increased average $PM_{2.5}$ concentrations were possibly due to enhanced source contributions from sulfate and secondary nitrate by increased coal consumption in the residential sector in neighboring areas. The $PM_{2.5}$ concentrations and contributions of secondary nitrate and sulfate in Tianjin, China, increased considerably due to various coal combustion processes, including household stoves for heating and cooking in the residential sector during the second week of February 2020 (Dai et al., 2021a). (Shen et al., 2021) reported that as the containment measures continued in northern China, the increased stay-at-home period resulted in more coal consumption in the residential sector during February 2020.

3.2. Source apportionment

The overall progress of the study from the stage after the monthly $PM_{2.5}$ concentration comparison is schematically presented in Fig. S4. We found differences in meteorological conditions for 2019 and 2020. VC decreased from 1438 m^2/s to 1300 m^2/s during January 2020 compared to 2019. However, VC increased from 1431 m^2/s to 1672 m^2/s and from 1440 m^2/s to 1878 m^2/s, respectively, during February and March 2020 compared to 2019. Since this study aims to analyze the transboundary impact of $PM_{2.5}$ sources due to the decrease in anthropogenic activity in the early stage of the COVID-19 outbreak, we applied DN-PMF to source apportionment in Seoul. DN-PMF was performed by normalizing with average VC for that entire study period, i.e., January–March and not monthly average VCs. DN-PMF using the hourly compositional data measured in Seoul resolved ten factors contributing to $PM_{2.5,}$ including secondary nitrate, sulfate, mobile, biomass burning, coal combustion, mining industry, soil, metallurgical industry, oil combustion, and district heating and incineration. The base results derived from the DN-PMF were constrained based on the prior information, and the source contributions used in this study were constrained results. Factor profiles and contributions resolved from DN-PMF are shown in Fig. S5. The narrow DISP interval for a specific species indicates minor rotational ambiguity, suggesting stably assigned solutions within the factor. Three sources (sulfate, coal combustion, and district heating and incineration) were associated with coal combustion are explained as follows.

The first factor resolved from DN-PMF characterized by high loadings of SO_4^{2-} (70%) and NH_4^+ (44%) was identified as primary sulfate (hereafter referred to as sulfate). SO_4^{2-} (70%) and NH_4^+ in sulfate profile show high concentrations with narrow DISP intervals. Sulfate contributed the most to $PM_{2.5}$ concentration, accounting for 26%. Given the relatively low humidity, cold temperature, and weak radiation in the winter, sulfate was likely emitted from coal combustion in a residential stove for heating and cooking. Particulate matter emitted from coal-burning at low temperatures was more oxidized, explaining the high contributions of sulfate during winter despite atmospheric conditions unfavorable to the secondary aerosol formation (Dai et al., 2018). Dai et al., 2019a showed that residential stoves burning briquette or chunk coal emit significant amounts of primary sulfate through laboratory tests. When residential coal is burned in a stove, sulfur is oxidized to SO_2 and SO_3. These two sulfur oxides can be interconverted. At low

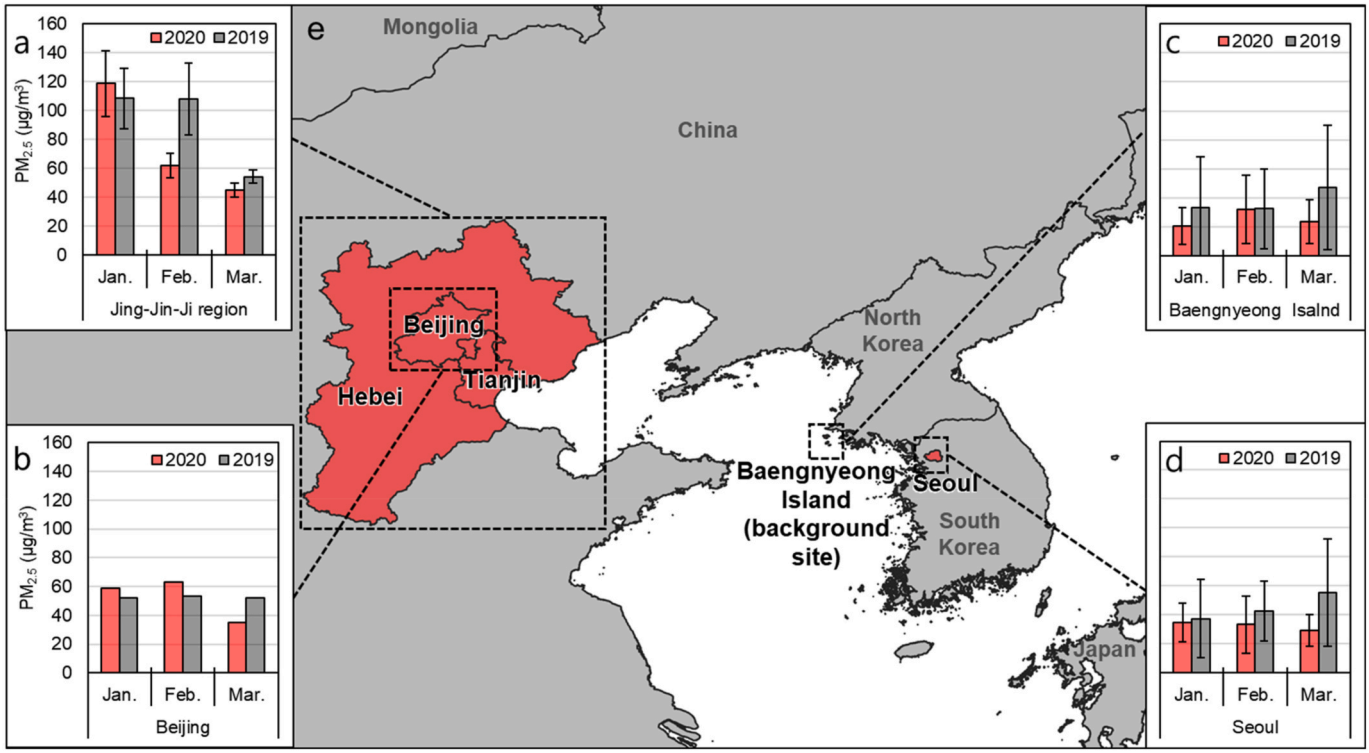

Fig. 1. Monthly average of $PM_{2.5}$ concentrations in China and Korea from January to March in 2019 and 2020. (a) Jing-Jin-Ji region (BTH). (b) Beijing. (c) Baengnyeong Island. (d) Seoul. The figure compares the average monthly concentration of $PM_{2.5}$ in 2020 compared to 2019. Error bars of Seoul and Baengnyeong Island indicate the standard deviations (SDs) of the observed hourly data. The error bars of the BTH indicate the SDs of $PM_{2.5}$ concentrations measured at monitoring stations in Beijing, Tianjin, and Hebei provinces. (e) Map of ground-based $PM_{2.5}$ monitoring regions. The dashed box indicates the BTH, Beijing, Baengnyeong Island, and Seoul.

temperatures below 500 °C, the conversion reaction from SO_2 to SO_3 is dominant (Cullis and Mulcahy, 1972). Therefore, the oxidized sulfur from the low-temperature combustion of the stove is mostly emitted in the form of SO_3 rather than SO_2. The emitted SO_3 forms H_2SO_4 with H_2O and then reacts with ammonia to form $(NH_4)_2SO_4$. This process rapidly proceeds after the primary emission of SO_3, which differs from secondary sulfate formation during non-heating periods of relatively high humidity. The PSCF results of sulfate show that potential source locations were mainly northeast and north China and the Shandong peninsula (Fig. S6). (Dai et al., 2019; X. Li et al., 2019) reported that a major source of sulfate in northern China is low-temperature based residential coal combustion in a stove for heating and cooking during the heating period (from October to March). The correlations between sulfate and coal-related sources (coal combustion, district heating and incineration) are poor (sulfate vs. coal-fired: $R^2 = 0.016$, sulfate vs. district heating and incineration: $R^2 = 0.18$) (Fig. S7). These results mean that DN-PMF properly solved the independent factors hidden in the original data. If the correlations between the factors of DN-PMF are good, it means that too many factors are solved. As discussed in section 3, sulfate and the other coal combustion-related sources in this study are based on different combustion conditions, which are low-temperature combustion in residential stoves that emit sulfate, high-temperature combustion in coal-boilers or coal-fired power plants that emit As, and high-temperature combustion from district heating systems that emit Cl^-.

The fifth factor that explained most of the variations of As (66%) and Pb (55%) was interpreted as coal combustion. As and Pb are well-known indicators of coal combustion (Smith, 2006; Wang et al., 2006). The narrow DISP intervals of As, Pb, OC, and EC supported that this factor was coal combustion, including high-temperature processes in coal-boilers and coal-fired power plants. The fifth factor is also a source mixing all the types of coal combustion used in residential stoves and district heating mentioned above. The CBPF plots of coal combustion show high probability values with all wind speeds from the NW direction (Fig. S8) of high $PM_{2.5}$ emissions areas by residential coal (Fig. S1).

The seventh factor most explained the Cl^- variance (72%) in the DN-PMF profile and was interpreted as district heating and incineration. Cl^- is an indicator of high-temperature combustion-based coal combustion-based coal burning (X. Li et al., 2019; Yu et al., 2013). In northern China, coal-based centralized heating systems that supply hot water to residential, public, and workplace buildings through high-temperature combustion are used by the government for official district heating, mainly from October to March. In the SMA, there was no official coal-based district heating system or power plant, and power plants have been using LNG and renewable energy, such as fuel cells and solar power. The PSCF results of the seventh factor show that potential source locations were mainly the Shandong peninsula, north China, and Mongolia (Fig. S9). The seventh factor also show high concentrations and narrow DISP intervals for Cl^- and OC. As these chemical species are emitted in large quantities from waste incineration (Li et al., 2019; Liu et al., 2018), the seventh factor was partially mixed with local waste incineration. During the study period, the CBPF plot of the seventh factor show high probability values mainly in the direction range from northwest to south (Fig. S10), where several municipal waste incineration facilities were located (Fig. S11). These supported that this seventh factor was locally affected by municipal waste incinerators in the SMA.

The Supplementary Material (Text S4) provided explanations for other sources. The $PM_{2.5}$ concentrations reconstructed by the constrained version and base version correlated well with the observed $PM_{2.5}$ concentrations with coefficients of determination (r^2) of 0.972 and 0.975, respectively (Fig. S12).

3.3. Monthly comparison of $PM_{2.5}$ sources identified in Seoul

We statistically analyzed changes in $PM_{2.5}$ concentrations and source contributions from January to March in Seoul in 2019 and 2020 using the Mann-Whitney *U* test (Fig. 2). The monthly analysis results show that $PM_{2.5}$ concentration statistically significantly decreased from 55.4 to 29.3 μg/m^3 (−47%) in Seoul during March 2020 compared to 2019 (Table S2) (after this, "statistically significantly" is referred to as "significant"). Similar to this reduction, the average contributions of sulfate and secondary nitrate decreased significantly from 16.7 to 6.93 μg/m^3 (−59%) and 17.3 to 7.98 μg/m^3 (−54%) ($p < 0.001$, respectively) in Seoul during March 2020 compared to 2019. The key drivers for the reductions in $PM_{2.5}$ concentrations (−26.1 μg/m^3) were sulfate (−9.77 μg/m^3) and secondary nitrate (−9.32 μg/m^3), accounting for 37% and 36%, respectively during March 2020. The PSCF results show that potential source locations of sulfate and secondary nitrate were concentrated in the Shandong peninsula, north China, and Mongolia in March 2019 (Fig. S6, Fig. S13). However, the potential source locations of sulfate in the Shandong peninsula disappeared in March 2020. These results show that China's emission reduction was associated with the massive reductions in the contributions of these sources (sulfate and secondary nitrate) identified in Seoul. The reductions of these sources were greater in the observation days of backward trajectory cluster 3 (C3) passing over north China compared to the total in March (Fig. S14). The average $PM_{2.5}$ concentration and average contributions of sulfate and secondary nitrate decreased significantly (Mann-Whitney *U* test, $p < 0.001$) from 81.7 to 28.3 μg/m^3 (−65%), 29.9 to 6.26 μg/m^3 (−79%), and 23.3 to 8.49 μg/m^3 (−64%), respectively during the C3 observation days. The reductions during the C3 observation days were greatest compared to those during the other cluster observation days (Fig. S15). These results support that north China played an important role in Korea's air quality.

With respect to coal combustion, the average contribution decreased significantly (Mann-Whitney *U* test, $p < 0.001$) from 1.85 to 1.34 μg/m^3 (−28%) (Fig. 2, Table S2) during February 2020 compared to 2019. Korea had reduced total PM emissions by 39% (2503 tons) from December 2019 to March 2020 compared to the same period of the previous year by implementing the seasonal fine dust management program such as shutting down 38 coal-fired power plants (Ministry of Environment Republic of Korea, 2020a). Most of South Korea's large coal-fired power plants (>5000 MW capacity) are located in western South Korea (Fig. S16). The proportion of cluster 4 (C4) of backward trajectories, which was closer to western South Korea during February 2020 compared to 2019, increased from 2.1% to 28% (Fig. S14). These results indicate that emission reductions from coal-fired power plants in Korea lowered the contribution of coal combustion during February 2020. On the other hand, the average contributions of coal combustion and sulfate increased significantly from 2.61 to 4.00 μg/m^3 (+53%) and from 7.40 to 10.7 μg/m^3 (+45%), respectively ($p < 0.001$, respectively) during January 2020 compared to 2019. This result indicates that the increase in residential coal consumption based on low-temperature combustion increased in China. Coal consumption in the residential sector increased by 30%–40% in China during the period from January 24 to February 8, 2020, compared to the period immediately preceding it owing to the increased duration of stay-at-home periods. The PSCF results show that the potential source locations of coal combustion and

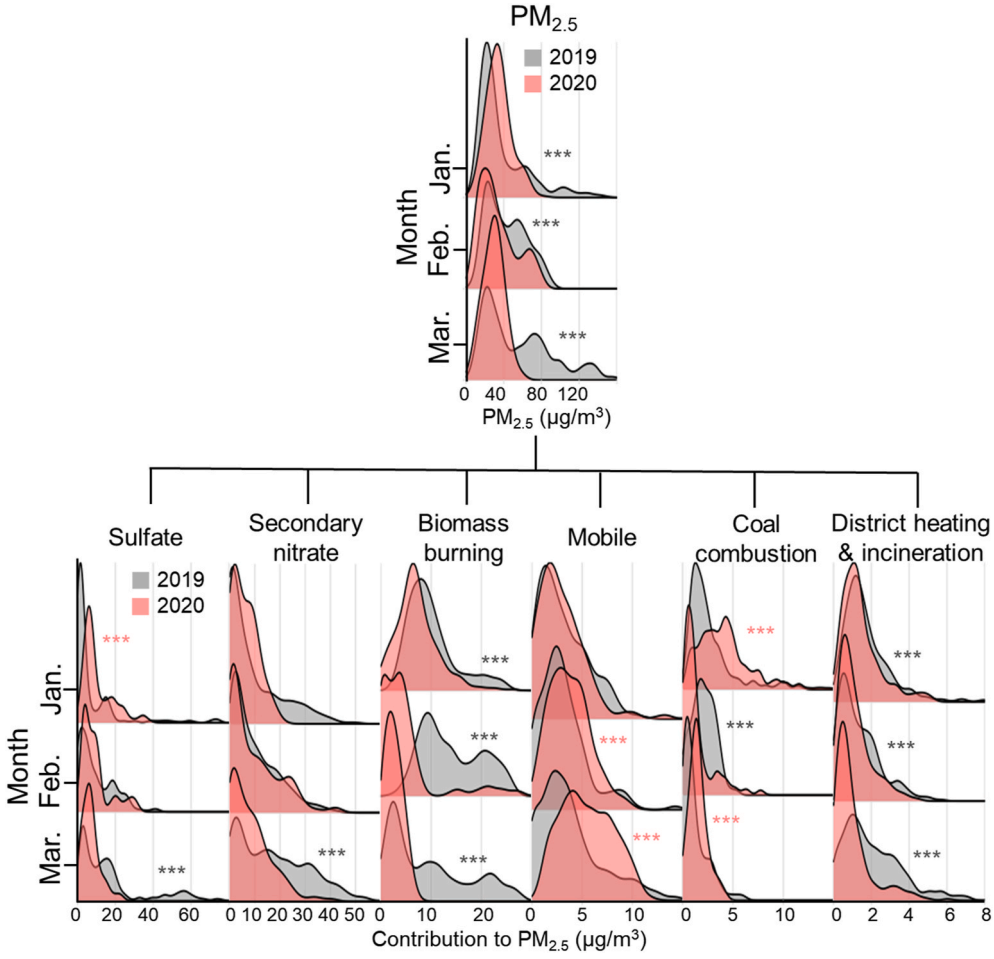

Fig. 2. Probability density function of $PM_{2.5}$ concentrations and sources contributions.The figure compares the $PM_{2.5}$ concentrations and sources contributions in 2020 compared to 2019. ***: $p < 0.001$. **: $p < 0.01$. *: $p < 0.05$. The error bars indicate the SDs.

sulfate were mainly north and central areas of China in January 2019 (Fig. S6, Fig. S17). However, most of the potential source locations disappeared during January 2020, and northeast China and surrounding areas were found as potential source locations. In addition to the extended stay-at-home period by China's COVID-19 measures, the heating degree-days in Jilin and Liaoning Provinces in northeast China increased during January 2020 compared to 2019 (Fig. S18), indicating that more residential coals for heating were needed at these potential source locations.

The average monthly contributions of biomass burning decreased significantly (Mann-Whitney U test, $p < 0.001$) not only in February and March but also during January (January: −2.92 μg/m^3 (−29%), February: −8.49 μg/m^3 (−65%), March: −7.12 μg/m^3 (−75%)) in Seoul during 2020 compared to 2019 (Fig. 2). According to China's Air Pollution Action Plan and regular media reports on May 2020, straw burning has been strongly regulated since 2020 and postponed in northeastern China, including the BTH, until March because of COVID-19. The PSCF results of biomass burning show that potential source locations were mainly the north and central areas of China and Mongolia during January–March 2019, but most potential source locations disappeared during 2020 (Fig. S19). Also, the CBPF plots of biomass burning show high probability values with wind directions from the Incheon (SW) and Gyeonggi Province (NW, NE) burning wood and crops residues (Ryou et al., 2018), but most disappeared in 2020 (Fig. S20). Korea's Ministry of Environment strongly prohibited the illegal open burning of crop residue and agricultural waste from December 2019 to March 2020 (Ministry of Environment Republic of Korea, 2020b). These results indicate that the combined effects of the two countries' emission regulations and China's COVID-19 lockdown measures reduced biomass burning contributions in Seoul.

The average monthly contributions of district heating and incineration decreased significantly (Mann-Whitney U test, $p < 0.001$) not only in February and March but also in January (January: −0.338 μg/m^3 (−20%), February: −0.169 μg/m^3 (−13%), March: −1.05 μg/m^3 (−52%)) compared to 2019 (Fig. 2, Table S2). The CBPF plot of district heating and incineration shows high probability values with wind directions (NW, W, SW) (Fig. S10) coming from multiple municipal waste incinerators and industrial complexes, which indicate the local source locations (Fig. S11). The PSCF results of district heating and incineration show that potential source locations were mainly the Shandong peninsula, north China, and Mongolia during 2019, but most potential source locations disappeared during 2020 (Fig. S9). Considering the increase in coal-based residential heating during the lockdown, this result may be due to reduced heating in public and workplace buildings.

The monthly average mobile contribution increased significantly (Mann-Whitney U test, $p < 0.001$) from 3.75 to 5.48 μg/m^3 (+46%) in Seoul in March 2020 compared to 2019 (Fig. 2). The short-distance traffic volume of personal transport on Korean highways increased significantly during 2020 compared to 2019 due to a decrease in the demand for public transportation (Korea Transport Institute, 2020). The daily traffic volume on the Han River Bridge in the center of Seoul increased from 1707 thousand vehicles/day to 1780 thousand vehicles/day (+4.3%) during March 2020 compared to 2019 (Fig. S21). The CBPF plot of mobile emissions factor shows high probability values with wind directions (S, SE, E) (Fig. S22) coming from the center of Seoul and roadway areas during March 2020 (Fig. S1). The personal transport share increased from 35.6% to 44.2%, and the traffic volume during commuting time increased due to the decrease in public transport in the SMA in February and March 2020 (Samsung Traffic Safety Research Institute, 2020).

The diel pattern of mobile source shows that the contribution increased during February and March 2020 compared to 2019 mainly during rush hour (7 a.m.–9 a.m., 5 p.m.–7 p.m.) and weekdays (Fig. S23). The traffic volume at the interchanges (IC) increased in Seoul during February–March 2020 compared to 2019 (Fig. S24), indicating increased personal transport commuting between Seoul and outside areas. These results supported the increased mobile traffic locally enhanced mobile contribution in Seoul during commuting time.

3.4. Transboundary impact of $PM_{2.5}$ source identified in Seoul

The contributions of $PM_{2.5}$ sources were assessed by increases or decreases, but the local and transboundary impacts related to these changes remain unclear. In general, air quality models are widely used to analyze the local and transboundary impact of air pollutants. However, air pollutant emissions have changed rapidly in China during the early stage of the COVID-19, and obtaining an emissions inventory for this period is difficult and highly uncertain (Kim et al., 2021). As an alternative to air quality modeling, this study analyzed synoptic meteorological patterns to evaluate local stagnation and long-range transport of air pollutants. Based on synoptic meteorological analyses, we investigated three episodes that most clearly revealed transboundary (episodes 1 and 2) and local (episode 3) impacts of $PM_{2.5}$ sources (Figs. S25–S27). Each episode was selected pairwise for the same period in 2020 and 2019. We defined episodes 1 and 2 as successive days with meteorological conditions favorable to long-range transport of air pollutants from China to Korea under westerly winds (episode 1: February 14–15 in 2020 and 2019, episode 2: March 2–6 in 2020 and 2019). To identify the local impact of $PM_{2.5}$ sources, we defined successive days with more distinct atmospheric stagnation in the SMA as episode 3 during 2020 compared to 2019 (episode 3: March 25–26 in 2020 and 2019). We analyzed changes in source contributions, including NO_2, O_3, MLH, wind direction, humidity, and traffic volume in Seoul during each episode to comprehensively evaluate the effects of atmospheric oxidation, meteorology, and emissions.

Episode 1 (February 14–15, 2020) showed the transboundary impact, which increased $PM_{2.5}$ concentrations and sources contributions compared to 2019. Meteorological conditions were favorable to the long-range transport of air pollutants in both years (Fig. S25). Backward trajectory analysis shows air masses originating from northeastern China in both years, which were characterized as Mongolian origin in 2019 (Fig. S28). VC decreased slightly from 1460 m^2/s to 1296 m^2/s (−13%) during 2020 compared to 2019, showing that episode 1 in 2020 was relatively more unfavorable to local dispersion.

The average contributions of primary sources (biomass burning, coal combustion, mining, and metallurgical industry) decreased in Seoul (Fig. 3a). (He et al., 2021)) reported that industrial activity declined in China during the early stage of the COVID-19 outbreak compared to 2019, and the decline in the mining industry activity was more remarkable than in other industrial sectors. Straw burning has been delayed in China until March 2020 due to the COVID-19 outbreak. Decreases in coal combustion contribution were likely due to decreases in the overall coal consumption of high-temperature combustion systems such as coal-fired power plants, industrial coal boilers, and district heating, despite an increase in residential coal consumption from January 2020.

In contrast, the average $PM_{2.5}$ concentration and average contributions of sulfate and secondary nitrate considerably increased from 29.1 to 58.6 μg/m^3 (+101%), 0.541–27.0 μg/m^3 (+4886%), and 5.31–17.3 μg/m^3 (+226%), respectively during episode 1 compared to 2019. The $PM_{2.5}$ concentrations and contributions of sulfate and secondary nitrate in Tianjin, China, increased significantly due to the residential coal combustion (Dai et al., 2021a) during the week including the first day of Episode 1 (7–14 February 2020). China's COVID-19 measures extended the stay-at-home period during February 2020, leading to more residential coal consumption in northern China. Given the dramatic decline in traffic volumes and industrial activities in China during COVID-19, NO_x emissions for secondary nitrate formation were most likely attributable to residential coal combustion. These results suggest that residential coal combustion in northern China enhanced sulfate and secondary nitrate contributions identified in Seoul by long-range transport, thereby elevating $PM_{2.5}$ concentration. Similar behaviors of

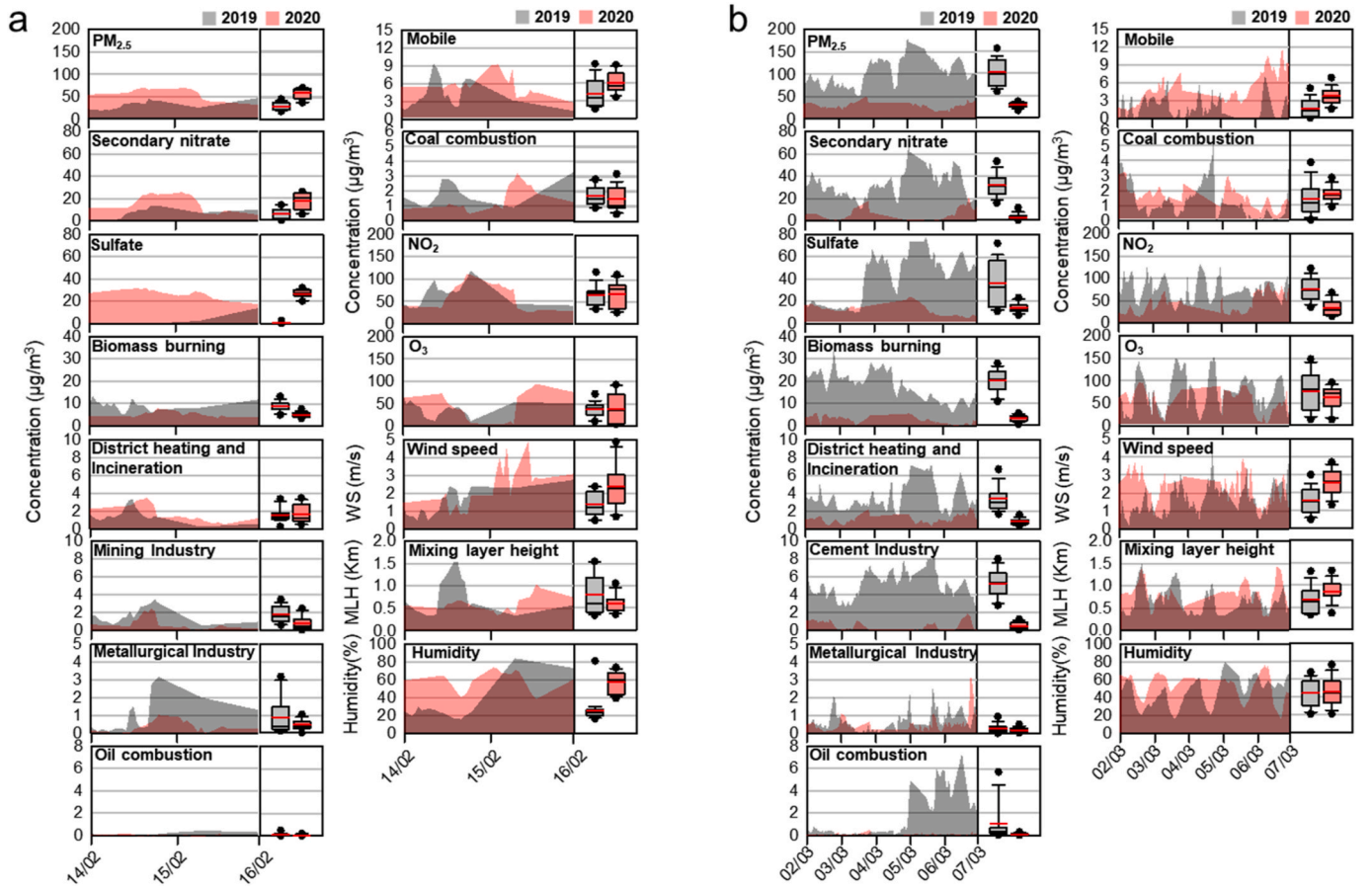

Fig. 3. Transboundary impacts on $PM_{2.5}$ concentration and source contributions in Seoul during the early stage of the COVID-19 outbreak in China. (a) Minimum effect (episode 1, left panel). (b) Maximum effect (episode 2, right panel).

sulfate and secondary nitrate were confirmed in the change in the average contribution in March in section 3.3. Also, similar behaviors are more evident during episode 2, which is more favorable for long-distance transport than during episode 1. This characteristic supports that both sources were emitted from residential coal and were affected by transboundary impacts.

Episode 2 (March 2–5, 2020) showed the transboundary impact of maximally reduced $PM_{2.5}$ concentrations and source contributions compared to 2019 (Fig. 3b). Meteorological conditions were favorable to the long-range transport of air pollutants from China to Korea under strong northwest winds in both years (Fig. S26). Backward trajectory analysis shows that most air masses originated from northeastern China, suggesting that long-range transports were dominant in both years (Fig. S28). VC decreased from 2272 m^2/s to 1088 m^2/s (+108%) during 2020 compared to 2019, indicating that episode 2 in 2020 was relatively more favorable to local dispersion. The average $PM_{2.5}$ concentration and average contributions of secondary nitrate and sulfate reduced sharply from 102 to 28.3 $\mu g/m^3$ (−72%), 31.3 to 2.41 $\mu g/m^3$ (−92%), and 36.3 to 14.4 $\mu g/m^3$ (−60%), respectively during episode 2 compared to 2019 (Fig. 3b). Also, the average contributions of most primary emission sources (biomass burning, district heating and incineration, mining industry, metallurgical industry, and oil combustion) decreased compared to 2019. China's emission reduction was maximally reflected in the sources identified in Seoul, explicitly showing the reduceable $PM_{2.5}$ concentration by transboundary impact. However, the average contributions of mobile increased from 1.60 to 3.68 $\mu g/m^3$ (+130%) (Fig. 3b). As mentioned earlier, the personal transport share in the SMA in February and March 2020 increased from 35.6% to 44.2%, and the traffic volume increased due to the decrease in public transport during the commuting time (Samsung Traffic Safety Research Institute, 2020). The enhanced mobile contributions were possibly due to the local impact, which was more evident in episode 3.

3.5. *Local impacts of $PM_{2.5}$ source identified in Seoul*

Episode 3 (March 25–26, 2020) revealed the local impact of $PM_{2.5}$ sources under meteorological conditions of increasing local stagnation compared to 2019 (Fig. S27). Backward trajectory analysis shows that air masses were stagnant on the Korean peninsula in 2020 compared to 2019. VC increased slightly from 1864 m^2/s to 2101 m^2/s (−11%) during 2020 compared to 2019, showing that episode 3 in 2020 was relatively more unfavorable to local dispersion. The average $PM_{2.5}$ concentration decreased from 36.8 to 34.9 $\mu g/m^3$ (−5.2%) during episode 3 compared to 2019, but still exceeded the 24-h National Ambient Air Quality Standards of South Korea (35 $\mu g/m^3$) (Fig. 4). While most source contributions decreased compared to 2019, mobile and coal combustion contributions increased from 3.57 to 7.80 (+118%) and 0.298–2.25 $\mu g/m^3$ (+656%), respectively. Air masses were stagnant on the southwestern peninsula (Fig. S28), where large-scale coal-fired power plants were densely located (Fig. S16). The daily traffic volumes in Seoul did not noticeably decrease during episode 3 compared to 2019 despite the social distancing period (2020: 9723 thousand vehicles/day, 2019: 9595 thousand vehicles/day) (Fig. S29). However, the day before Episode 31 (March 24), daily traffic volume increased noticeably from 8346 thousand vehicles/day to 9583 thousand vehicles/day (+13%) during 2020 compared to 2019. The primary air pollutants emitted from this increase in traffic volume probably accumulated during episode 3. These results suggest the local impact of atmospheric stagnation on the Korean Peninsula elevated the contribution of mobile and coal combustion in Seoul.

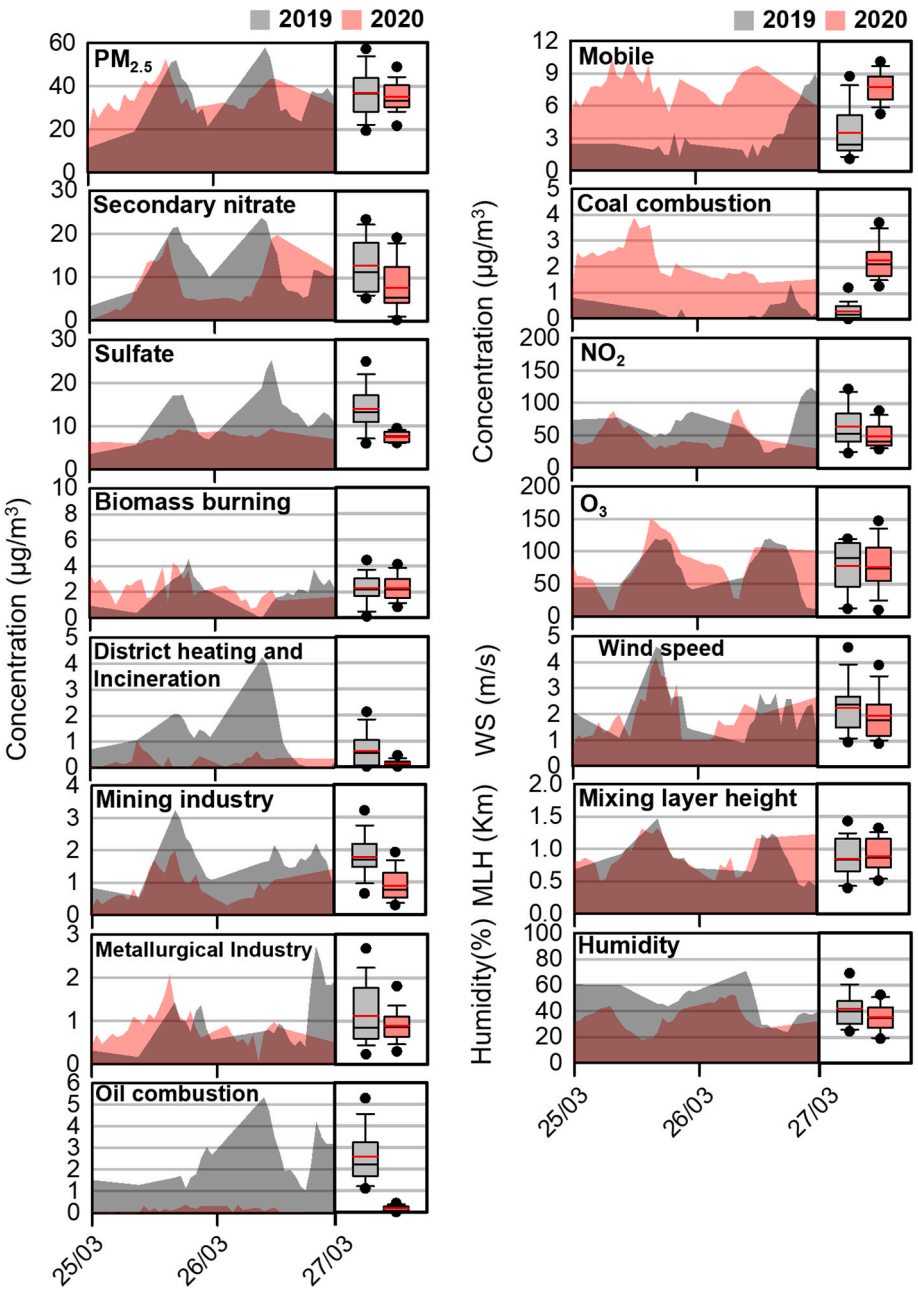

Fig. 4. Local impact on $PM_{2.5}$ concentration and source contributions in Seoul during the early stage of COVID-19 outbreak in China. Local impact (episode 3).

4. Conclusions

This study is the first to analyze the effects of the drastic decrease in anthropogenic activities during the early stage COVID-19 outbreak in China on the $PM_{2.5}$ source type identified in Seoul. We conducted this study according to the schematic diagram in Fig. S4 and separated the local and transboundary impacts of $PM_{2.5}$ sources. First, the contributions of $PM_{2.5}$ sources were evaluated, and compared monthly from January to March 2020 with corresponding 2019 dates by normalizing differences in meteorological conditions using DN-PMF. The monthly average of $PM_{2.5}$ concentration and contributions of sulfate, secondary nitrate, biomass burning, and district heating and incineration in Seoul in March 2020 decreased significantly (−47%, −59%, −54%, −75%, and −52%, respectively) ($p < 0.001$) compared to 2019. We also evaluated the contributions of $PM_{2.5}$ sources compared to 2019 during three episodes showing the different meteorological conditions. Episodes 1 and 2 revealed transboundary impacts and were related to reduced anthropogenic emissions and accumulated primary pollutants in Northeast China. Anthropogenic emissions, except for the residential sector, decreased, but primary air pollutants accumulated by residential coal combustion enhanced secondary aerosol formation. Thus, the contributions of sulfate and secondary nitrate increased in Seoul during episode 1 but then decreased maximally with other primary sources (biomass burning, district heating and incineration, mining industry, metallurgical industry, and oil combustion) during episode 2 under meteorological conditions favorable to long-range transport. Local impact was demonstrated by atmospheric stagnation during episode 3. Meteorological condition unfavorable to local dispersion elevated the contributions of mobile and coal combustion and further contributed to $PM_{2.5}$ high concentration events (HCE). These impacts evaluated by only three episodes are likely to contain quantitative uncertainties. However, DN-PMF lowered the uncertainties of atmospheric dilution affecting $PM_{2.5}$ source apportionment. Also, analyzing similar meteorological episodes lowered uncertainties due to atmospheric stagnation and long-

range transport. Therefore, the method combining DN-PMF and meteorological episodes minimized the uncertainties in evaluating local and transboundary impacts, thereby separating each impact, the goal of this study.

Through this study, indirectly evaluating the air quality improvement level that can be achieved in the downwind area for maximally reducing the source emissions from China was possible. We also confirmed that the contributions of $PM_{2.5}$ sources identified in Seoul decreased as affected by air quality policies. It is difficult to separate the effects of air quality policies and China's lockdown. However, this study clearly shows the local and transboundary impacts of $PM_{2.5}$ sources separately, which still contributed to HCEs even after air quality improved in Seoul. Consequently, we identified the sources that require domestic management and cross-country cooperation. We suggest the need for comprehensive cooperation on air quality management in Northeast Asia to policymakers by separating the local and transboundary impacts of $PM_{2.5}$ sources.

As confirmed in this study, Korea and China can be called a "breathing community" that shares the same air. In Korea and China, various policies have recently been pursued to reduce the primary air pollutant emissions, revealing their effects (Cheng et al., 2018; Y. Kim et al., 2020; Lee et al., 2019; Zhao et al., 2019). However, this study suggests that if no strong emission controls exist in an upwind area, such as regional containment measures, management of local emission sources alone may not improve air quality in a downwind area. To effectively improve air quality in the future, cooperation in Northeast Asia on secondary aerosol formation and management of local emission sources in individual countries are both necessary.

Credit author statement

Youngkwon Kim: Investigation, Visualization, Writing – original draft preparation, Writing – review & editing. Seung-Muk Yi: Conceptualization, Methodology, Supervision, Writing – review & editing. Kwonho Jeon: Conceptualization, Investigation, Supervision, Writing – review & editing. Hye-Jung Shin: Methodology, Investigation, Writing – review & editing. Sang-Woo Kim: Methodology, Investigation, Supervision, Writing – review & editing. Kyuseok Shim: Methodology, Investigation, Visualization, Writing – original draft preparation, Writing – review & editing. Jieun Park: Investigation, Writing – review & editing. Philip K. Hopke: Result interpretation, Writing – review & editing.

Declaration of competing interest

The authors declare that they have no known competing financial interests or personal relationships that could have appeared to influence the work reported in this paper.

Acknowledgments

This work was supported by the National Institute of Environmental Research (NIER) of the Ministry of Environment under grant No. NIER-2021-04-02-211 and the Ministry of Education of the Republic of Korea and the National Research Foundation of Korea (BK21 FOUR 5199990214126). The authors gratefully acknowledge the National Institute of Environmental Research (NIER) of the Ministry of Environment for providing the $PM_{2.5}$ chemical speciation data (NIER-2021-03-03-001).

Appendix A. Supplementary data

Supplementary data to this article can be found online at https://doi.org/10.1016/j.apr.2022.101510.

References

Ali, S.M., Malik, F., Anjum, M.S., Siddiqui, G.F., Anwar, M.N., Lam, S.S., Nizami, A.S., Khokhar, M.F., 2021. Exploring the linkage between $PM_{2.5}$ levels and COVID-19 spread and its implications for socio-economic circles. Environ. Res. 193, 110421 https://doi.org/10.1016/j.envres.2020.110421.

Apte, J.S., Brauer, M., Cohen, A.J., Ezzati, M., Pope, C.A., 2018. Ambient $PM_{2.5}$ reduces global and regional life expectancy. Environ. Sci. Technol. Lett. 5, 546–551. https://doi.org/10.1021/acs.estlett.8b00360.

Ashrafi, K.H., Shafipour, M., Kamalan, H., 2009. Estimating temporal and seasonal variation of ventilation coefficients. Int. J. Environ. Res. 3, 637–644. https://doi.org/10.22059/IJER.2010.79.

Bae, C., Kim, B.-U., Kim, H.C., Yoo, C., Kim, S., 2019. Long-range transport influence on key chemical components of $PM_{2.5}$ in the Seoul metropolitan area, South Korea, during the years 2012–2016. Atmosphere 11, 48. https://doi.org/10.3390/atmos11010048.

Bey, I., Jacob, D.J., Logan, J.A., Yantosca, R.M., 2001. Asian chemical outflow to the Pacific in spring: origins, pathways, and budgets. J. Geophys. Res. Atmos. 106, 23097–23113. https://doi.org/10.1029/2001JD000806.

Borro, M., Di Girolamo, P., Gentile, G., De Luca, O., Preissner, R., Marcolongo, A., Ferracuti, S., Simmaco, M., 2020. Evidence-based considerations exploring relations between sars-cov-2 pandemic and air pollution: involvement of $PM_{2.5}$-mediated up-regulation of the viral receptor ace-2. Int. J. Environ. Res. Publ. Health 17, 1–13. https://doi.org/10.3390/ijerph17155573.

Briz, Á., Carolina, R., Sapiña, B., Serrano, Á., 2022. A city-level analysis of $PM_{2.5}$ pollution, climate and COVID-19 early spread in Spain. J. Environ. Health Sci. Eng. 20, 395–403. https://doi.org/10.1007/s40201-022-00786-2.

Chang, Y., Huang, R.J., Ge, X., Huang, X., Hu, J., Duan, Y., Zou, Z., Liu, X., Lehmann, M. F., 2020. Puzzling haze events in China during the coronavirus (COVID-19) shutdown. Geophys. Res. Lett. 47, 1–11. https://doi.org/10.1029/2020GL088533.

Cheng, J., Su, J., Cui, T., Li, X., Dong, X., Sun, F., Yang, Y., Tong, D., Zheng, Y., Li, J., Zhang, Q., He, K., 2018. Dominant role of emission reduction in $PM_{2.5}$ air quality improvement in Beijing during 2013–2017: a model-based decomposition analysis. Atmos. Chem. Phys. Discuss. 1–31. https://doi.org/10.5194/acp-2018-1145.

Choi, J., Park, R.J., Lee, H., Lee, S., Jo, D.S., Jeong, J.I., Henze, D.K., Woo, J., Ban, S., Lee, M., Lim, C., Park, M., Shin, H.J., Cho, S., Peterson, D., Song, C., 2019. Impacts of local vs. trans-boundary emissions from different sectors on $PM_{2.5}$ exposure in South Korea during the KORUS-AQ campaign. Atmos. Environ. 203, 196–205. https://doi.org/10.1016/j.atmosenv.2019.02.008.

Cohen, A.J., Brauer, M., Burnett, R., Anderson, H.R., Frostad, J., Estep, K., Balakrishnan, K., Brunekreef, B., Dandona, L., Dandona, R., Feigin, V., Freedman, G., Hubbell, B., Jobling, A., Kan, H., Knibbs, L., Liu, Y., Martin, R., Morawska, L., Pope, C.A., Shin, H., Straif, K., Shaddick, G., Thomas, M., van Dingenen, R., van Donkelaar, A., Vos, T., Murray, C.J.L., Forouzanfar, M.H., 2017. Estimates and 25-year trends of the global burden of disease attributable to ambient air pollution: an analysis of data from the Global Burden of Diseases Study 2015. Lancet 389, 1907–1918. https://doi.org/10.1016/S0140-6736(17)30505-6.

Cui, Y., Ji, D., Maenhaut, W., Gao, W., Zhang, R., Wang, Y., 2020. Levels and sources of hourly $PM_{2.5}$-related elements during the control period of the COVID-19 pandemic at a rural site between Beijing and Tianjin. Sci. Total Environ. 744, 140840 https://doi.org/10.1016/j.scitotenv.2020.140840.

Cullis, C.F., Mulcahy, M.F.R., 1972. The kinetics of combustion of gaseous sulphur compounds. Combust. Flame 18 (2), 225–292. https://doi.org/10.1016/S0010-2180(72)80139-1.

Czy, B., 2019. Efficiency of the EU environmental policy in struggling with fine particulate matter ($PM_{2.5}$): how agriculture makes a difference? Sustainability 11 (18), 4984. https://doi.org/10.3390/su11184984, 2019.

Dai, Q., Bi, X., Liu, B., Li, L., Ding, J., Song, W., Bi, S., Schulze, B.C., Song, C., Wu, J., Zhang, Y., Feng, Y., Hopke, P.K., 2018. Chemical nature of $PM_{2.5}$ and PM_{10} in Xi'an, China: insights into primary emissions and secondary particle formation. Environ. Pollut,. 240, 155–166. https://doi.org/10.1016/j.envpol.2018.04.111.

Dai, Q., Bi, X., Song, W., Li, T., Liu, B., Ding, J., Xu, J., Song, C., Yang, N., Schulze, B.C., Zhang, Y., Feng, Y., Hopke, P.K., 2019. Residential coal combustion as a source of primary sulfate in Xi'an, China. Atmos. Environ. 196, 66–76. https://doi.org/10.1016/j.atmosenv.2018.10.002.

Dai, Q., Liu, B., Bi, X., Wu, J., Liang, D., Zhang, Y., Feng, Y., Hopke, P.K., 2020. Dispersion normalized PMF provides insights into the significant changes in source contributions to $PM_{2.5}$ after the COVID-19 outbreak. Environ. Sci. Technol. 54 (16), 9917–9927. https://doi.org/10.1021/acs.est.0c02776, 2020.

Dai, Q., Ding, J., Hou, L., Li, L., Cai, Z., Liu, B., Song, C., Bi, X., Wu, J., Zhang, Y., Feng, Y., Hopke, P.K., 2021a. Haze episodes before and during the COVID-19 shutdown in Tianjin, China: contribution of fireworks and residential burning. Environ. Pollut,. 286, 117252 https://doi.org/10.1016/j.envpol.2021.117252.

Dai, Q., Ding, J., Song, C., Liu, B., Bi, X., Wu, J., Zhang, Y., Feng, Y., Hopke, P.K., 2021b. Changes in source contributions to particle number concentrations after the COVID-19 outbreak: insights from a dispersion normalized PMF. Sci. Total Environ. 759 https://doi.org/10.1016/j.scitotenv.2020.143548.

Fan, H., Zhao, C., Yang, Y., 2020. A comprehensive analysis of the spatio-temporal variation of urban air pollution in China during 2014 – 2018. Atmos. Environ. 220, 117066 https://doi.org/10.1016/j.atmosenv.2019.117066.

Han, B.S., Park, K., Kwak, K.H., Park, S.B., Jin, H.G., Moon, S., Kim, J.W., Baik, J.J., 2020. Air quality change in Seoul, South Korea under covid-19 social distancing: focusing on $PM_{2.5}$. Int. J. Environ. Res. Publ. Health 17, 1–12. https://doi.org/10.3390/ijerph17176208.

He, C., Yang, L., Cai, B., Ruan, Q., Hong, S., Wang, Z., 2021. Impacts of the COVID-19 event on the NO_x emissions of key polluting enterprises in China. Appl. Energy 281, 116042. https://doi.org/10.1016/j.apenergy.2020.116042.

Helsel, D.R., Hirsch, R.M., Ryberg, K.R., Archfield, S.A., Gilroy, E.J., 2002. Statistical Methods in Water Resources. https://doi.org/10.3133/tm4A3. Report (USGS Numbered Series).

Heo, J.B., Hopke, P.K., Yi, S.M., 2009. Source apportionment of $PM_{2.5}$ in seoul, korea. Atmos. Chem. Phys. 9, 4957–4971. https://doi.org/10.5194/acp-9-4957-2009.

Hersbach, H., Bell, B., Berrisford, P., Hirahara, S., Horányi, A., Muñoz-Sabater, J., Nicolas, J., Peubey, C., Radu, R., Schepers, D., Simmons, A., Soci, C., Abdalla, S., Abellan, X., Balsamo, G., Bechtold, P., Biavati, G., Bidlot, J., Bonavita, M., De Chiara, G., Dahlgren, P., Dee, D., Diamantakis, M., Dragani, R., Flemming, J., Forbes, R., Fuentes, M., Geer, A., Haimberger, L., Healy, S., Hogan, R.J., Hólm, E., Janisková, M., Keeley, S., Laloyaux, P., Lopez, P., Lupu, C., Radnoti, G., de Rosnay, P., Rozum, I., Vamborg, F., Villaume, S., Thépaut, J.N., 2020. The ERA5 global reanalysis. Q. J. R. Meteorol. Soc. 146, 1999–2049. https://doi.org/10.1002/qj.3803.

Hopke, P.K., 2016. Review of receptor modeling methods for source apportionment. J. Air Waste Manag. Assoc. 66, 237–259. https://doi.org/10.1080/10962247.2016.1140693.

Kim, Y.P., Lee, G., 2018. Trend of air quality in Seoul: policy and science. Aerosol Air Qual. Res. 9 https://doi.org/10.4209/aaqr.2018.03.0081, 2018.

Kim, H., Zhang, Q., Bae, G., Kim, J.Y., Lee, S.B., 2017a. Sources and atmospheric processing of winter aerosols in Seoul, Korea: insights from real-time measurements using a high-resolution aerosol mass spectrometer 2009–2033. Atmos. Chem. Phys. 17, 2009–2033. https://doi.org/10.5194/acp-17-2009-2017, 2017.

Kim, H.C., Kim, S., Kim, B.U., Jin, C.S., Hong, S., Park, R., Son, S.W., Bae, C., Bae, M.A., Song, C.K., Stein, A., 2017b. Recent increase of surface particulate matter concentrations in the Seoul Metropolitan Area, Korea. Sci. Rep. 7, 1–7. https://doi.org/10.1038/s41598-017-05092-8.

Kim, H., Zhang, Q., Sun, Y., 2020. Measurement report: characterization of severe spring haze episodes and influences of long-range transport in the Seoul metropolitan area in March 2019. Atmos. Chem. Phys. 20, 11527–11550. https://doi.org/10.5194/acp-20-11527-2020.

Kim, H.C., Kim, S., Cohen, M., Bae, C., Lee, D., Saylor, R., Bae, M., Kim, E., Kim, B., Yoon, J., Stein, A., 2021. Quantitative Assessment of Changes in Surface Particulate Matter Concentrations and Precursor Emissions over China during the COVID-19 Pandemic and Their Implications for Chinese Economic Activity 10065–10080.

Kruskal, W.H., Wallis, W.A., 1952. Use of ranks in one-criterion variance analysis. J. Am. Stat. Assoc. 47, 583–621. https://doi.org/10.2307/2280779.

Le, T., Wang, Y., Liu, L., Yang, J., Yung, Y.L., Li, G., Seinfeld, J.H., 2020. Unexpected air pollution with marked emission reductions during the COVID-19 outbreak in China, 1979 Science 7431. https://doi.org/10.1126/science.abb7431. eabb7431.

Lee, E., Chan, C.K., Paatero, P., 1999. Application of positive matrix factorization in source apportionment of particulate pollutants in Hong Kong. Atmos. Environ. 33, 3201–3212. https://doi.org/10.1016/S1352-2310(99)00113-2.

Lee, D., Choi, J.Y., Myoung, J., Kim, O., Park, J., Shin, H.J., Ban, S.J., Park, H.J., Nam, K. P., 2019. Analysis of a severe $PM_{2.5}$ episode in the Seoul metropolitan area in South Korea from 27 February to 7 March 2019: focused on estimation of domestic and foreign contribution. Atmosphere 10, 1–12. https://doi.org/10.3390/ATMOS10120756.

Li, H., Gao, P., Ni, H., 2019. Emission characteristics of parent and halogenated PAHs in simulated municipal solid waste incineration. Sci. Total Environ. 665, 11–17. https://doi.org/10.1016/j.scitotenv.2019.02.002.

Liu, Yiming, Fan, Q., Chen, X., Zhao, J., Ling, Z., Hong, Y., Li, W., 2018. Modeling the impact of chlorine emissions from coal combustion and prescribed waste incineration on tropospheric ozone formation in China 2709–2724. Atmos. Chem. Phys. 18, 2709–2724. https://doi.org/10.5194/acp-18-2709-2018, 2018.

Maji, K.J., Ye, W.F., Arora, M., Shiva Nagendra, S.M., 2018. $PM_{2.5}$-related health and economic loss assessment for 338 Chinese cities. Environ. Int. 121, 392–403. https://doi.org/10.1016/j.envint.2018.09.024.

Mann, H.B., Whitney, D.R., 1947. On a test of whether one of two random variables is stochastically larger than the other. Ann. Math. Stat. 18 (1), 50–60. https://doi.org/10.1214/aoms/1177730491. March, 1947.

Ming, W., Zhou, Z., Ai, H., Bi, H., Zhong, Y., 2020. COVID-19 and air quality: evidence from China COVID-19 and air quality: evidence from China. Emerg. Mark. Finance Trade 56, 2422–2442. https://doi.org/10.1080/1540496X.2020.1790353.

Ministry of Environment Republic of Korea, 2019. Summary Report of the 4th Stage (2013– 2017) LTP Project. https://www.me.go.kr/home/file/readDownloadFile.do?fileId=184686&fileSeq=1.

Ministry of Environment Republic of Korea, 2020a. Report on the Reduction of the Concentration of PM by the Seasonal Management in Korea. https://han.gl/zp8fe.

Ministry of Environment Republic of Korea, 2020b. Regulation of Agricultural Waste Incineration. http://me.go.kr/wonju/web/board/read.do?menuId=1056&boardId=1422440&boardMasterId=258&condition.hideCate=1.

Park, D.H., Kim, S.W., Kim, M.H., Yeo, H., Park, S.S., Nishizawa, T., Shimizu, A., Kim, C. H., 2021. Impacts of local versus long-range transported aerosols on PM_{10} concentrations in Seoul, Korea: an estimate based on 11-year PM_{10} and lidar observations. Sci. Total Environ. 750, 141739 https://doi.org/10.1016/j.scitotenv.2020.141739.

Pitiranggon, M., Johnson, S., Haney, J., Eisl, H., Ito, K., 2021. Long-term trends in local and transported $PM_{2.5}$ pollution in New York City. Atmos. Environ. 248, 118238 https://doi.org/10.1016/j.atmosenv.2021.118238.

Rovetta, A., Castaldo, L., 2020. Relationships between demographic, geographic, and environmental statistics and the spread of novel coronavirus disease (COVID-19) in Italy. Cureus 2. https://doi.org/10.7759/cureus.11397.

Ryou, H. gon, Heo, J., Kim, S.Y., 2018. Source apportionment of PM_{10} and $PM_{2.5}$ air pollution, and possible impacts of study characteristics in South Korea. Environ. Pollut,. 240, 963–972. https://doi.org/10.1016/j.envpol.2018.03.066.

Samsung Traffic Safety Research Institute, 2020. The Master Series of Traffic Accident Prevention, No. 7. Sts samsungfire.com/information/regulations/asn/asn_202028_07/asn_issue2.html.

Shen, H., Shen, G., Chen, Y., Russell, A.G., Hu, Y., Duan, X., Meng, W., Xu, Y., Yun, X., Lyu, B., Zhao, S., Hakami, A., Guo, J., Tao, S., Smith, K.R., 2021. Increased air pollution exposure among the Chinese population during the national quarantine in 2020. Nat. Human Behav. 5, 239–246. https://doi.org/10.1038/s41562-020-01018-z.

Smith, K., 2006. TEM study of $PM_{2.5}$ emitted from coal and tire combustion in a thermal power station. Environ. Sci. Technol. 40 (20), 6235–6240. https://doi.org/10.1021/es060423m, 2006.

Transport Institute, Korea, 2020. Analysis and Response to the Impact of COVID-19 on the Transportation Sector. https://www.koti.re.kr/main/covid19/). Korea Transport Institute special edition. https://www.koti.re.kr/main/covid19/) 265, 5–16.

Tu, W., Tang, H., Chen, F., Wei, Y., Xu, T., Liao, K., Xiang, N., Shi, G., Li, Q., Feng, Z., 2020. Epidemic update and risk assessment of 2019 novel coronavirus — China, January 28, 2020. China CDC Weekly 2, 83–86. https://doi.org/10.46234/ccdcw2020.024.

Uria-tellaetxe, I., Carslaw, D.C., 2014. Conditional bivariate probability function for source identification. Environ. Model. Software 59, 1–9. https://doi.org/10.1016/j.envsoft.2014.05.002.

US EPA, 2014. EPA Positive Matrix Factorization (PMF) 5.0 Fundamentals and User Guide. https://www.epa.gov/air-research/epa-positive-matrix-factorization-50-fundamentals-and-user-guide.

Wang, X., Bi, X., Sheng, G., Fu, J., 2006. Chemical composition and sources of PM_{10} and $PM_{2.5}$ aerosols in guangzhou, China 425–439. Environ. Monit. Assess. 119, 425–439. https://doi.org/10.1007/s10661-005-9034-3, 2006.

Wang, Y., Yuan, Y., Wang, Q., Liu, C.G., Zhi, Q., Cao, J., 2020. Changes in air quality related to the control of coronavirus in China: implications for traffic and industrial emissions. Sci. Total Environ. 731, 139133 https://doi.org/10.1016/j.scitotenv.2020.139133.

Wetchayont, P., Hayasaka, T., Khatri, P., 2021. Air quality improvement during COVID-19 lockdown in bangkok metropolitan, Thailand: effect of the long-range. Trans. Air Pollut. 21, 1–16.

Xie, Y., Dai, H., Dong, H., Hanaoka, T., Masui, T., 2016. Economic impacts from $PM_{2.5}$ pollution-related health effects in China: a provincial-level analysis. Environ. Sci. Technol. 50, 4836–4843. https://doi.org/10.1021/acs.est.5b05576.

Xie, Y., Dai, H., Zhang, Y., Wu, Y., Hanaoka, T., Masui, T., 2019. Comparison of health and economic impacts of $PM_{2.5}$ and ozone pollution in China. Environ. Int. 130, 104881 https://doi.org/10.1016/j.envint.2019.05.075.

Yang, X., Wang, Y., Zhao, C., Fan, H., Yang, Y., Chi, Y., 2022. Health risk and disease burden attributable to long-term global fine-mode particles. Chemosphere 287, 132435. https://doi.org/10.1016/j.chemosphere.2021.132435.

Yu, L., Wang, G., Zhang, R., Zhang, L., Song, Y., Wu, B., Li, X., An, K., Chu, J., 2013. Characterization and source apportionment of $PM_{2.5}$ in an urban environment in beijing 574–583. Aerosol Air Qual. Res. 13, 574–583. https://doi.org/10.4209/aaqr.2012.07.0192.

Zhang, Q., Jiang, X., Tong, D., Davis, S.J., Zhao, H., Geng, G., Feng, T., Zheng, B., Lu, Z., Streets, D.G., Ni, R., Brauer, M., Van Donkelaar, A., Martin, R.V., Huo, H., Liu, Z., Pan, D., Kan, H., Yan, Y., Lin, J., He, K., Guan, D., 2017. Transboundary health impacts of transported global air pollution and international trade. Nature 543, 705–709. https://doi.org/10.1038/nature21712.

Zhang, Q., Zheng, Y., Tong, D., Shao, M., Wang, S., Zhang, Y., Xu, X., Wang, J., He, H., Liu, W., Ding, Y., Lei, Y., Li, J., Wang, Z., Zhang, X., Wang, Y., Cheng, J., Liu, Y., Shi, Q., Yan, L., Geng, G., Hong, C., Li, M., Liu, F., Zheng, B., Cao, J., Ding, A., Gao, J., Fu, Q., Huo, J., Liu, B., Liu, Z., Yang, F., He, K., Hao, J., 2019. Drivers of improved $PM_{2.5}$ air quality in China from 2013 to 2017. Proc. Natl. Acad. Sci. U.S.A. 116, 24463–24469. https://doi.org/10.1073/pnas.1907956116.

Zhang, Q., Pan, Y., He, Y., Walters, W.W., Ni, Q., Liu, X., Xu, G., 2021. Substantial nitrogen oxides emission reduction from China due to COVID-19 and its impact on surface ozone and aerosol pollution. Sci. Total Environ. 753, 142238 https://doi.org/10.1016/j.scitotenv.2020.142238.

Zhao, C., Fan, H., Yang, Y., Sun, Y., 2019. Toward understanding the differences of $PM_{2.5}$ characteristics among five toward understanding the differences of $PM_{2.5}$ characteristics among five China urban cities. Asia-Pacific J Atmos Sci 56, 493–502. https://doi.org/10.1007/s13143-019-00125-w, 2020.

Zhao, Y., Zhang, K., Xu, X., Shen, H., Zhu, X., Zhang, Y., Hu, Y., Shen, G., 2020. Substantial changes in nitrogen dioxide and ozone after excluding meteorological impacts during the COVID-19 outbreak in mainland China. Environ. Sci. Technol. Lett. 7, 402–408. https://doi.org/10.1021/acs.estlett.0c00304.